JOURNAL OF PHYSICAL ORGANIC CHEMISTRY
J. Phys. Org. Chem. 2007; **20:** 422–430
Published online in Wiley InterScience
(www.interscience.wiley.com) DOI: 10.1002/poc.1167

Physical image *vs* structure relation: part 12 – structure of 2,2,5,5-tetramethyl-dihydro-furan-3-one oxime and its protonated forms through isomerization and NMR spectra†

Ryszard B. Nazarski*

Department of Organic Chemistry, Institute of Chemistry, University of Łódź, Narutowicza 68, 90-136 Łódź, Poland

Received 15 September 2006; revised 26 October 2006; accepted 15 January 2007

ABSTRACT: The study of an isomeric **A/B** mixture of the title oxime **1**, by photolytic or thermal *E*,*Z*-isomerization and NMR measurement including $^1H\{^1H\}$-NOE difference spectra, led to assignment of the *E* configuration to its predominating form **A**. The $^1H/^{13}C$ data were interpreted in terms of steric overcrowding of both forms, especially of the thermolabile photoproduct **B**. Four classical (empirical) NMR methods of elucidating the oxime geometry were critically tested on these results. Unexpected vapor-phase photoconversion **A**→**B** in the window glass-filtered solar UV and spectroscopic findings on their protonated states were discussed, as well. The kinetically controlled formation of the *N*-protonated species (*Z*)-$\mathbf{5}^+$ was proved experimentally. In addition, some ^1H NMR assignments reported for structurally similar systems were rationalized (**3** and **4**) or revised (**1** and **7–9**) with the GIAO-DFT(B3LYP) and/or GIAO-HF calculational results. Copyright © 2007 John Wiley & Sons, Ltd.
Supplementary electronic material for this paper is available in Wiley Interscience at http://www.interscience.wiley.com/jpages/0894–3230/suppmat/

KEYWORDS: gas-phase photoreactions; *E*/Z-isomerization; solar UV; protonated oximes; solvent effects; nuclear Overhauser effect; LIS analysis; GIAO method

INTRODUCTION

The NMR spectroscopy is an extremely powerful tool for studying organic species. It enables an elucidation of the structure and conformational preferences of such objects. However, some problems can be occasionally encountered during the subtle spectroscopic effects interpretations, especially when only a single approach is applied.

In our studies on sterically crowded rings, oxime **1** was prepared following the literature procedure.[1] After vacuum sublimation in a Pyrex vessel exposed accidentally to solar rays, the product appeared to be a mixture of two isomers (major **A**: minor **B** ≈ 85:15), in contrast to data reported by Latovskaya *et al.* [1] According to these authors only one form of **1** (henceforth abbreviated as **A**) was formed under such conditions (except for a Pyrex/sunlight coincidence), to which the *Z* configuration[2] was assigned,[1,3] based on the ^1H NMR results obtained with $Eu(dpm)_3$ as a lanthanide shift reagent (LSR).

To species **A** of mp *ca.* 398 K,[1,4] the only one form of **1** described until now, the *E* geometry was assigned earlier[4b] from the outcome of its reaction with concentrated sulfuric acid; the normal Beckmann rearrangement was assumed. However **1**, as derivative of an α-alkoxy imine, undergoes[5] heterolytic fragmentation[5,6] under such conditions and no structural information is available. On contrary, analysis of steric interactions between oximino (hydroxyimino) and *gem*-diCH_3 fragments in both isomers allowed to anticipate that the more stable form **A** has the *E* geometry.

The rearrangements in oxime systems are known as their unstable forms undergo usually conversion into stable counterparts (*Z*-to-*E* isomerism) thermally, by a prolonged exposure to daylight or chemically, for example, with use of protic acids. By contrast, a higher energy (shorter wavelength) UV irradiation through quartz and/or special filters must be applied for reverse processes conducted as major reactions (or beside the competing photo-Beckmann rearrangement) in non-polar media, usually deoxygenated just before use.[7] Recently, the solid-state photoisomerization was detected even for molecules trapped in low-temperature matrices and a reversible photoproduct formation was found leading to an achievement of the photostationary state (PSS).[8] By changing the wavelength of UV irradiation, $\lambda > 295$ nm *vs* $\lambda > 335$ nm, the equilibrium composition could be altered,[9] in line with the above generalities. Dependence

**Correspondence to:* R. B. Nazarski, Department of Organic Chemistry, University of Łódź, Narutowicza 68, 90-136 Łódź, Poland.
E-mail: rynaz@chemul.uni.lodz.pl
†For Part 11, see Ref. 36.

of the PSS mixtures on UV wavelength (λ254 *vs* 366 nm) was found also for conjugated ketoximes (accompanied by the solvent effect)[10] and used for preparative photoreactions.[7c,11]

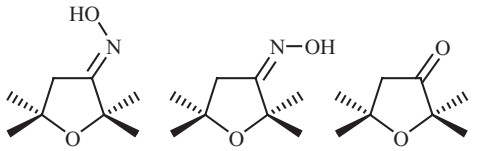

(*E*)-**1** (*Z*)-**1** **2**

Therefore, an assignment[1,3] of *Z* geometry to **A** seemed to be incorrect, and we decided to re-establish its structure. This work presents results from isomerization and NMR studies on both isomers of **1** in the mixture, which led unequivocally to the *E* configuration for **A**. Having a well-known **A/B** mixture in hand, enabled us to test additionally the reliability and present-time usefulness of some classical NMR spectra-based methods[12] of empirical nature as tools for elucidating the oximino geometry in oximes. Among these results, a spectroscopically proved formation of the *N*-protonated states (*Z*)-**1** under kinetical control conditions is of great interest, in the light of some recent works on the Beckmann rearrangement.[13] Present experimental findings were fully confirmed by high-level quantum mechanical calculations of isomer ratios and $^{1}H/^{13}C$ NMR chemical shifts (using the GIAO method,[14] both at the HF and at DFT level of theory). To the best of our knowledge, this is the first application of such a comprehensive approach for oximes. The observed photoisomerization **A**→**B** in sun's rays filtered through a window glass is also worthy of mention, in view of reported persistence of unconjugated ketoximes to Pyrex-filtered UV radiation.[7a]

RESULTS AND DISCUSSION

Isomerization of oxime 1 and analysis of steric interactions

Isomeric mixtures of a slightly different composition (**A**:**B** ≈ 85:15; by ^{1}H NMR) from a few sublimations of the crude product **1** *in vacuo*, were subjected to thermal analysis. It was found that **B** undergoes reisomerization above its mp_1 at *ca.* 348–354 K leading to formation of **A** ($mp_2 \sim 399$ K).[15] Conversion **B**→**A** proceeded also in the presence of catalytic amounts of protic acid. This process was observed very well in NMR spectra taken in commercial $CDCl_3$, contaminated usually with traces of DCl.[16] By contrast, the crude **1** contained ~99% of **A** and its recrystallization led to the stereochemical purity enhancement.

Above facts indicated that an **A/B** mixture richer with a thermally unstable photoproduct **B** was formed by sunlight radiation filtered through the soda-lime/borosilicate glasses (photochemical *E*-to-*Z* isomerization). Indeed, it can be supposed that this accidental exposure to sun's UV rays was equivalent to 366-nm irradiation with a high-pressure Hg lamp.[17] To the best of our knowledge, no reports were in the literature on the photoisomerization of oximes in the gas phase. Instead, photolysis of the parent ketone **2** at 313 nm, through Pyrex in methanol or pentane, was interpreted in terms of an initial Norrish type I cleavage of the more highly substituted C—C bond adjacent to the C=O group.[18]

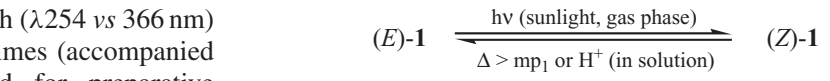

(*E*)-**1** $\underset{\Delta > mp_1 \text{ or } H^+ \text{ (in solution)}}{\overset{h\nu \text{ (sunlight, gas phase)}}{\rightleftharpoons}}$ (*Z*)-**1**

Scheme 1. Isomerization of the oxime **1**

For aliphatic ketimines >C=N~Y one should expect a predominance of sterically preferred form with Y *syn* to the least substituted α-carbon atom, from classical concept of the great significance of steric bulkiness.[12e,19] Moreover, thermal isomerization of oximes fails entirely to produce detectable amounts of unfavorable forms.[12a] Accordingly, all the foregoing rearrangements of **1** can be rationalized by photolytic **A**→**B** and thermal or chemical **B**→**A** processes (Scheme 1). So, we assigned the *E* configuration to the more thermochemically stable form **A**, in opposition to earlier LSR results.[1,3] This proposal was justified in the further NMR studies.

Spectroscopic investigations

In order to establish independently the geometry of both isomers **1**, their **A/B** mixture was analyzed by using four classical NMR techniques of empirical nature (i-iv);[12] the resulting chemical shifts δ_Xs and diagnostic differences are listed in Tables 1–3.

(i) **DMSO solution method**. It was originally found that replacement of *syn*- and *anti*-CH_3 groups in acetone oxime by larger alkyls produces in DMSO-d_6 an upfield (low-frequency) and a downfield shift of diagnostic δ_H(OH)s, respectively.[12a] Shifts of this kind observed for **1** allowed signal assignment for **A** and **B** to species of the geometry *E* and *Z*, respectively. These δ_H(OH)s were found insensitive to concentration, most likely due to strong solvent-solute (as a monomeric entity) intermolecular H-bonding.[20] As expected, this dependency was found with CCl_4 and C_6D_6 (Table 1). Similar NMR effects assigned to the *tert*-butyl hindered formation of the H-bond $S^+O^- \cdots HO$—N, were reported previously.[21] Substantial difference δ^E_H(OH)—δ^Z_H(OH) of 0.17 ppm for **1** and downfield shift of both δ_Hs should be also noted, in view of those found for other ketoximes.[12a,22] The latter data are indicative of the large overcrowding in oximes **1**.

DOI: 10.1002/poc

Table 1. ^{1}H NMR data for **1** in the **A/B** (*E*/*Z*) ≈ 85:15 mixture, δ_H, ppm[a]

Entry	Solvent	2-C(CH$_3$)$_2$, s		4-CH$_2$, s		5-C(CH$_3$)$_2$, s		OH, s	
		anti (**A**)	*syn* (**B**)	*syn* (**A**)	*anti* (**B**)	*syn* (**A**)	*anti* (**B**)	**A**	**B**
1	DMSO-d_6	1.26	1.39	2.59	2.48_5	1.21	1.21	10.56	10.39
2	CCl_4[b]	1.34	1.48	2.68	2.55	1.30	1.30	9.48[c,d]	9.44[c,e]
3	$CDCl_3$	1.40	1.55	2.76	2.60_5	1.34	1.34	9.39[f,g]	[h]
4	C_6D_6	1.44	1.65	2.65	2.39	1.12_5	1.12_5	9.64[i,j]	9.56[i]
5	C_6D_6 + 2 mL HCl_{aq} vapor[k]	1.44	1.61	2.65	2.40[f]	1.12_5	1.09	8.94[f]	
6	C_6D_6 + 6 mL HCl_{aq} vapor[l]	1.44	1.55	2.64	2.45_5[m]	1.12	1.07	9.29	

[a] All signal assignments are based on the GIAO B3LYP/6-311+G(2*d*,*p*)//B3LYP/6-31G(*d*,*p*) results (*vide infra*). The words *syn* and *anti* indicate a spatial disposition of the particular group with respect to the hydroxyl unit of an oximino group.
[b] Data reported in Ref. 1 must include an error, because both *gem*-diCH$_3$ signals of (*E*)-**1** are listed as occurring at δ 1.28.
[c] Signals at 9.23
[d] and 9.18
[e] ppm, respectively, for different concentration.
[f] Broad.
[g] At 9.28 ppm for pure *E*.
[h] Not observed.
[i] One common very broad resonance signal at 9.60 ppm, under some circumstances.
[j] At 9.44 ± 0.10 ppm, for various solutions of the pure form *E*.
[k] About 10% of the *Z* species.
[l] About 9% of the *Z* species.
[m] Very broad.

Table 2. Solvent-induced shifts for oximes **1** (*E*/*Z* ≈ 85:15), δ_H, ppm[a]

		α-CH$_2$		β-CH$_3$[b]	
	CH$_n$ *vs* OH relation	$\Delta\delta$[c]	$\Delta\delta_s$[d]	$\Delta\delta$[c]	$\Delta\delta_s$[d]
CCl_4	—	0.13	—	0.14	—
C_6D_6	—	0.26	—	0.21	—
—	*syn*	—	−0.02	—	0.17
—	*anti*	—	−0.15	—	0.10

[a] Based on the data given in Table 1.
[b] For *gem*-diCH$_3$ groups in the position 2.
[c] $\Delta\delta = \delta_{syn} - \delta_{anti}$.
[d] $\Delta\delta_s = \delta_{C6D6} - \delta_{CCl4}$.

Table 3. ^{13}C NMR data and shift parameters for the conversion of **2** to **1** (*E*/*Z* ≈ 9:1), δ_C or $\Delta\delta_C$, ppm[a]

	(*E*)-**1**	(*Z*)-**1**	**2**
C2	80.10	80.21	80.45
C3	168.05	167.30	214.17
C4	39.46	43.86	48.22
C5	79.06	78.80	75.86
2-CH$_3$	30.05	26.39	26.32
5-CH$_3$	29.15	29.15	30.13
$\Delta_{\alpha-syn}$[b]	−8.8	−0.2	—
$\Delta_{\alpha-anti}$[b]	-0.3_5	−4.4	—
$\Delta_{\alpha-syn} - \Delta_{\alpha-anti}$	−8.4	4.1	—
$\delta_\alpha - \delta_\alpha^*$[b,c]	−8.8	−4.4	—

[a] See footnote a in Table 1.
[b] $\Delta_{\alpha-syn}$ ($\Delta_{\alpha-anti}$ or $\delta_\alpha - \delta_\alpha^*$) = $\delta_{oxime} - \delta_{ketone}$.
[c] For the CH$_2$ carbon nuclei in the position 4.

(ii) **Solvent-induced shift techniques** based on the use of magnetic anisotropy of the >C═N∼OH molecular unit ($\Delta\delta$) and aromatic-solvent induced shift (ASIS) effects ($\Delta\delta_s$) in the ^{1}H NMR spectra taken in CCl_4 and C_6D_6. All differences $\Delta\delta$ and $\Delta\delta_s$ for α-CH$_2$ protons in **1** (Table 2) agree with stereochemical relations established empirically by Karabatsos and Taller[12b] only on an assumption of the *E* isomer predominance. However, α *syn-anti* effects found for the voluminous *gem*-diCH$_3$ group in position 2 ($\Delta\delta > 0$, $\Delta\delta_s > 0$) are generally inconsistent with those reported for simple methyl ketoximes ($\Delta\delta \approx 0$, $\Delta\delta_s < 0$). The latter results strongly suggest a great influence of steric crowding in both isomers **1** on the oxime-aromatic solvent interactions. Very similar NMR spectroscopic picture was reported for aliphatic moieties in two carbocyclic structural analogues **4** (of unknown geometry) found in a practically identical molar ratio of 84:16 (in $CDCl_3$) with $\Delta\delta_H$s of 0.22 and 0.12 ppm for their CH$_3$ and OH protons, respectively.[23]

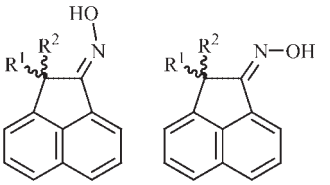

R^1 = H, R^2 = Me (*E*)-**3** (*Z*)-**3**
R^1 = R^2 = Me (*E*)-**4** (*Z*)-**4**

(iii) **Hydrochloric acid vapor method**. Since HCl is known to catalyze isomerization in oximes,[6a] this

DOI: 10.1002/poc

approach was applied with caution. Indeed, such a reaction was really found, however C-H signals due to both isomers **1** were easily identified in the ^{1}H NMR spectra taken in C_6D_6 with gradual acidification of the surrounding medium by bubbling repeatedly the same, but rather little known, amount of HCl_{aq} vapor through the solution (Table 1). In this technique, the upfield and downfield shifts of *α-syn* and *α-anti* signals occur, respectively,[12c,d] describing the time-average environments of the ^{1}H nuclei in protonated and non-protonated states of the oxime. Adequate *α* shifts were found for both forms, very small for **A** (−0.007 ppm) and large for **B** (+0.061 ppm) indicating for an equilibrium between (*Z*)-**1** and related ammonium salt (*Z*)-**5**$^+$Cl as a main phenomenon observed. Therefore, it was reasonable to assume the *N*-protonation[12c,13e,24] of (*Z*)-**1**, realized by a proton attack from the less hindered side (under kinetical control conditions), as proved experimentally.[25]

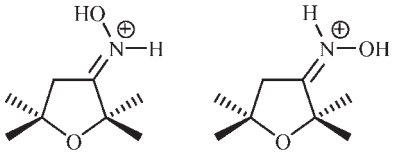

(*E*)-**5** (*Z*)-**5**

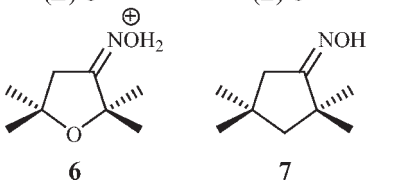

6 **7**

Substantial, not reported to date, upfield shift of the signal from remote *gem*-diCH_3 group in the position 5 was also interesting (Table 2), especially from a viewpoint of the structure of generated H^+-states. The initial formation of ammonium ions in a molecular mechanism postulated for the acid-catalyzed Beckmann rearrangement of oximes was discussed recently.[13] But, a competitive protonation of an oxygen atom giving rise to the *O*-states **6** was also considered,[12c,13a-c,e] since protonation occurs without any barrier (according to reported calculational results).[13a] Our finding of initial *N*-protonation of oxime **1** is in agreement with recent report by Blasco and co-workers based on the solid-state NMR data.[13f]

(iv) ***Syn-anti* effect technique.** Generally, ^{13}C NMR signals of both *α*-carbons in the system shift upfield on the oxime formation, with an effect for the *α-syn* C atom being considerably greater than for the *α-anti C*.[12e,f] The δ_Cs and shift parameters Δ_α measured for the **A/B** mixture and parent ketone **2** are given in Table 3. Differences $\Delta_{\alpha-\text{syn}}$ and $\Delta_{\alpha-anti}$ found for **2→1** indicate the *E* geometry for **A**. The shielding effect of C_α atoms proposed as a diagnostic tool for the *α*-diketone monooximes (δ_α–$\delta_\alpha{}^*$, where α^* stands for the ketone *α* atom),[26] exists also for the 4-CH_2 carbon in 1, but to a substantially lesser extent in relation to that reported for such diketone derivatives. Interestingly, the ($\Delta_{\alpha-syn}$–$\Delta_{\alpha-anti}$) difference for a strongly overcrowded form **B** is positive (+4.1 ppm) and much higher than an unique positive value of +1.1 ppm (or even only of +0.8 ppm) found for the large collection of ketoximes.[12f] Thus, present results fully confirm an earlier assumption that such differences are steric in origin.[12e,f]

(v) **NOE-based measurements.** Finally, modern ^{1}H 1D nuclear Overhauser enhancement (NOE) difference NMR spectra[27] were acquired for dilute solution of pure form **A** of **1** in DMSO-d_6 as a solvent of choice for oximes (in order to obtain the strong/sharp deuterium lock signal and narrow NOH lines, due to a sufficiently slow exchange rate of this type of protons in such hydrogen-bond acceptor medium).[27,28] Irradiation of the OH singlet caused a small enhancement of the *α*-CH_2 signal at 2.59 ppm. In contrast, a reverse experiment (saturation of an *α*-CH_2 transition) revealed a 1.3% NOE of a nearby *gem*-diCH_3 unit singlet and a 2.1% NOE of the OH line (at 1.21 and 10.56 ppm, respectively) indicating a close through-space connection between all these protons.[29] This proved unequivocally the *E* geometry of an analyzed form of oxime **1** and confirmed simultaneously the *syn*-OH arrangement assigned to its *β*-C$(CH_3)_2$ protons at 1.21 ppm.

Molecular modeling and Predicting the NMR Spectra

Overcrowded oximes 1, 3 and 4. Although the HF/6–31G(*d*,*p*) is a standard level for all studies on the NHR (or OH) group-containing systems or on the hyperconjugative stereoelectronic effects,[30] we attempted to take partially an electronic correlation into account. Accordingly, density functional theory (DFT) was used at the hybrid B3LYP level. In addition, standard Gibbs free-energy differences, ΔG°, between both forms of **1** were predicted in scaled frequency calculations[31] giving the isomer ratios *E*:*Z* of 95.1:4.9 and 97.1:2.9 for the basis sets 6–31G(*d*,*p*) and 6–31(+)G(*d*,*p*),[32,33] respectively (Table S2), in comparison with the observed **A**:**B** ≈ 85:15 (*vide infra*). The more extended basis, 6–311+G(2*d*,*p*),[34] was used in subsequent gauge independent atomic orbital (GIAO)[14] calculations of the chemical shieldings σ_Xs, to consider properly free electron pairs on heteroatoms. The NMR data computed in this way fully confirmed the foregoing *E*,*Z*-assignments (see Figure S2 for two possible assignments of the most diagnostic ^{13}C NMR signals). To the best of our knowledge, this kind of

DOI: 10.1002/poc

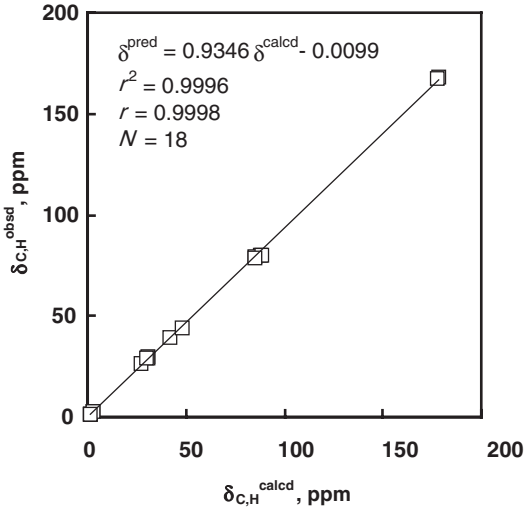

Figure 1. Scatter plot of a relation $\delta_{C,H}^{obsd}$ *vs* $\delta_{C,H}^{calcd}$ from the linear regression analysis of the GIAO/DFT-B3LYP/6-311+G(2*d*,*p*)//B3LYP/6-31G(*d*,*p*) results for both isomers of **1** (results from Tables S1 and S3).

calculations were not carried out before for oximes of such a molecular size. The antiperiplanar (*ap*, s-*trans*) rotamer about the single bond in the ═N—OH molecular unit was always preferentially found for **1** (Figure S1).

The scatter diagram and scaling equation of the type $\delta_{C,H}^{pred} = a\delta_{C,H}^{obsd} + b$ evaluated for both forms *E* and *Z* of **1** in $CDCl_3$ are given in Fig. 1.[35] In general, theoretical and real δ_Xs matched very well; $r(\delta_C) \geq 0.9998$, $r(\delta_C) \geq 0.9997$ and $r(\delta_H) \geq 0.9986$, respectively.[37] The strong correlation was found also for δ_Hs measured in CCl_4 and DMSO-d_6; $r(\delta_H) = 1.0000$ and $r(\delta_H) \geq 0.9971$ for *E* and *Z*, respectively, in both solvents. These statistical results can be regarded as the best proof of correctness of assignments given above. Moreover, such an excellent compatibility between NMR data observed and calculated for single isomers **1** indicates on their high conformational rigidity and overcrowding preventing an existence of the H-bonds resulting in their self-association, that is known to exist among the 'normal' (not sterically crowded) oximes.[12b]

The 0.983-scaled B3LYP/6–31G(*d*,*p*) approach[38] was used also for the structurally related oximes **3** and **4** affording $\Delta G^{\circ}_{298.15}$ of 0.18 and 4.01 kJ mol^{-1} in favor of (*E*)-**3** and (*Z*)-**4**, respectively (Table S2), in excellent agreement with the 1:1 and 16:84 ratios[23] evaluated from ^{1}H NMR spectra of their isomeric mixtures (most likely equilibrated in $CDCl_3$ solution, *vide supra*). According to the GIAO B3LYP/6–311+G(2*d*,*p*) results obtained for **4**, these planar molecules of C_s symmetry are responsible for *gem*-diCH_3 signals at 1.80_8 and 1.47_5 ppm, in line with reported δ_Hs 1.85 and 1.63 ppm; $\Delta\delta_H$s 0.33_3 *vs* 0.22 ppm. Analogous data $\Delta\delta_H(CDCl_3)$ for **1** and di-*tert*-butyl ketoxime (DtBK) are 0.24_1 *vs* 0.14 ppm and 0.19_3 *vs* 0.16[39] ppm, respectively (Table S3). Consequently, the value $\Delta\delta_H$ of 0.18 ppm can by tentatively recognized as the average *E*,*Z*-shielding difference typical of this sort of oximes due to an oximino group anisotropy, that is, deshielding of *gem*-diCH_3 protons attributable to the *syn* spatial proximity of an oxygen lone-pair electron density.[6b,7b] For both ring conformations of **1**, this difference is no doubt modified by the surrounding medium (especially by an aromatic solvent); the $\Delta\delta_H$ of 0.24_1 ppm GIAO-predicted *vs* 0.13–0.21 ppm observed experimentally in different solvents (Table 1).

An excellent compatibility of a relation δ_H^{calcd} *vs* δ_H^{obsd} for **3** and **4** with $r(\delta_H)$ 0.9990 [and for oximes **1**, **3** and **4**; $r(\delta_H)$ 0.9991] permitted to predict the ^{1}H NMR data for 2,2,4,4-tetramethyl-cyclopentanone oxime (**7**),[1] that is, the carbocyclic analogue of oxime **1**, only if its *E* geometry had previously been supposed (Table S3, Figure S3).[40] As above for (*Z*)-**1**, a large δ_H^{calcd} *vs* δ_H^{obsd} disagreement was found using the *Z* geometry assigned originally.[1] On the other hand, a high compatibility of energetics for **3** and **4** in the gaseous *vs* liquid phase suggests that the obtained **A/B** mixture of **1** (*E*:*Z* ≈ 85:15) does not represent the true equilibrium composition, because only ≤5% of (*Z*)-**1** was computed at both applied levels of theory (*vide supra*).

Protonated states of oxime 1. Similar calculational treatment was used for the *N*-protonated oximes **5** and *O*-protonated states **6** as the other possible H^+-derivatives of oxime **1**. In addition, the conformational equilibria must be considered for ammonium cations **5** due to the rotation around the N(H)—OH bond leading to different rotameric forms (Figure S4). Corresponding +*ac* and −*ac* forms were computed practically equivalent in energy because of an approximate planarity of these species. On the other hand, the stability of *sp* rotamers was found dependent on the theoretical levels applied. As to oxonium ions **6**, a large elongation of the N—O^+H_2 bond to 1.640 Å (or even to 1.680 Å) was computed for the (*E*)-**6** and (*Z*)-**6** isomers, respectively (Figure 2), in comparison to 1.551 Å found for such a distance in *O*-protonated formaldehyde oxime.[41] However, these high energy (in comparison to states **5**) structures **6** were localized as the true potential minima, in spite of simultaneous shortening of the C═N double bond [especially large for (Z)-**6**]. Calculational results for all the important H^+-species are listed in Table S4.

Unfortunately, the GIAO δ_H data showed that the used free-molecule approximation is rather not adequate for salt (*Z*)-**5**$^+Cl^-$. In fact, deshielding of all protons was predicted for its low-energy structures, whereas such a trend was found only for the CH_2 group in (*Z*)-**1** (Table 1, entries 4–6). However, an observed upfield shift of the ^{1}H NMR signal due to the *gem*-diCH_3 fragment in the position 5 was reproduced computationally quite well for the preferred −*ac* rotamer of (*Z*)-**5**$^+$. Also, expected differences in δ_Hs arising from the oximino group anisotropy were predicted correctly for all these H^+-species.

DOI: 10.1002/poc

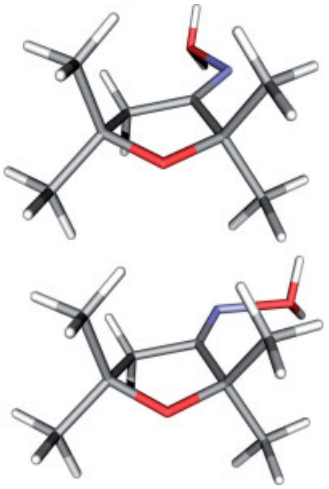

Figure 2. 3D views[52,53] of the HF/6-31G(*d*,*p*)-type geometries of the major *E* (top) and minor *Z* (bottom) isomers of the *O*-protonated state **6** revealing a large elongation of the N–O^+H_2 single bond (see text).

Possible explanation of failing the LIS method for oximes 1 and 7–9

As to the failure of Latovskaya *et al.* [1] in elucidating the geometry of **1** and structurally related oximes **7–9** by using LSRs, it did not arise from some imperfections inherent in the lanthanide-induced shift (LIS) method. It seems rather that authors adopted too simplified model of the LSR-substrate (LSR·S) complex, that is, the Ln^{3+} cation interacting solely with the nitrogen lone pair. However, an alternative binding with an oximino oxygen was found for the other oximes.[42] Moreover, the ^{1}H NMR data were analyzed only. Generally, it is most advisable to use the ^{1}H and ^{13}C data evaluated simultaneously for the same solution, in all LIS-based analyses of species with several Lewis-basic binding sites capable to interact with the Ln^{3+} ion.[43] Other aspects of the early (often erroneous) interpretations of such data were reviewed.[44] Recently, a novel approach to analyses of this kind was presented, in which both paramagnetic and diamagnetic LISs are normalized separately.[45]

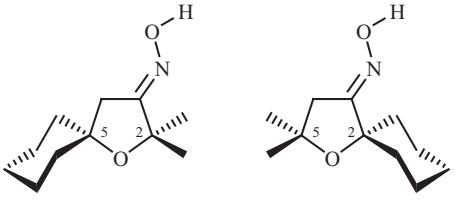

8 **9**

SUMMARY AND CONCLUSIONS

The study of an exocyclic C═N bond configuration in two stereoisomers of the title compound showed full agreement between results from experimental (isomerization, NMR) and theoretical (bulk approach) methods; its predominant more stable form **A** adopts the *E* geometry. The NMR-spectroscopic image rather not typical of the oximes was found for an **A/B** mixture, undoubtedly resulting from high overcrowding of its components. Indeed, the photoisomer (*Z*)-**1** is one of a few sterically unfavored ketoximes with an α quaternary carbon studied to date.

The first two of NMR techniques tested (i-ii, and LIS) are based on the subtle effects arising from solvent shifts, specific solvation or LSR·S complex formation. All these classical methods are reliable, but a good knowledge of the solute-solvent (or LSR interactions) is necessary for their application, especially in the case of the labor-consuming LIS method. But, adequate available datasets for oximes are not too wide, and serious problems occasionally may occur for overcrowded systems; especially this concerns the δ_H(OH)s for the single isomers in DMSO-d_6. The third method (iii) also works well but it is limited to the α group ^{1}H signals only. However, monitoring of the formed H^+-states of oximes is of great value. Undoubtedly, the last ^{13}C NMR technique (iv) is a classical method of choice because only solutions in $CDCl_3$ are used, but still requires both isomers to be measured. The later limitation is not valid for all modern non-empirical (NOE-based) methods. Among them, the NOE difference spectra proposed firstly by Heinisch and Holzer[27] seem to be the most valuable, especially recorded for degassed samples in DMSO-d_6.[29]

Generally, different and simultaneously independent experimental techniques and/or theoretical approaches should be applied in all stereochemical studies. In many cases, however, the most fruitful is parallel use of adequate computational calculations to model the structure and to compare statistically its observed *vs* calculated physical (especially spectroscopic) image. For instance, the GIAO / DFT-B3LYP/6–311+G(2*d*,*p*)//B3LYP/6–31G(*d*,*p*) method applied here was found to be sufficient for the oximes. In fact, the use of a locally-dense (mixed) basis sets approach afforded similar or even slightly worse results. As an environment of the $CDCl_3$ molecules does not modify seriously a solute geometry, the NMR spectra in this solvent are usually regarded as an useful starting point for any structural considerations concerning isolated molecules. Moreover, such a joint approach works also very well when pertinent physical data is available only for one of two isomers [see *e.g.,* NMR results for oxime (*E*)-**7**], in contrast to all the classical methods discussed above.

EXPERIMENTAL

General methods

The ^{1}H/^{13}C{^{1}H} NMR spectra were recorded in 5-mm OD tubes at ~294 K on a Varian Gemini 200 BB

DOI: 10.1002/poc

spectrometer at 199.98/50.29 MHz. For solutions in CCl_4, a coaxially situated 1.5-mm ID glass tube filled with D_2O was included to provide the deuterium lock signal. The 1D homonuclear differential NOE experiments were done for non-degassed solution[27] in DMSO-d_6 with the standard pulse sequence *noemul*, by using a Bruker AVANCE™ DRX 500 spectrometer operating at 500.13 MHz for ^{1}H (Centre of Molecular and Macromolecular Studies, Polish Academy of Sciences). Chemical shifts are reported in ppm from TMS as internal standard; δ_X 0.00 ppm. All deuterated solvents ($\geq$99.6 atom % D) were applied as received. Spectral-grade CCl_4 was distilled over P_4O_{10} through a Vigreux column. Other commercial solvents and reagent-grade chemicals were applied without any further treatment. Melting points were determined on a Boëtius hot-plate microscope and are uncorrected.

Synthesis of 2,2,5,5-tetramethyl-dihydrofuran-3-one oxime (1)

This compound was obtained *via* the literature procedure,[1] by direct oximation of ketone **2**[46] with a 20% excess of $NH_2OH{\cdot}HCl$ in refluxing EtOH-pyridine solution (3:1, v:v) for 3 h. After the normal work-up and recommended *sublimation* of the crude product (90% yield) under reduced pressure ($\sim$350 K/$\sim$80 Pa, all-Pyrex apparatus, exposure to bright window-glass-filtered solar rays) the crystalline isomeric mixtures were obtained [**A**:**B** ($\equiv$ *E:Z*) $\approx$ 85:15($\pm$1), by ^{1}H NMR] giving satisfactory analytical data. No significant change in the composition was found upon several-months standing.[15] Instead, *recrystallization* of the crude 1 provided its pure form **A** (>99.5% of *E*, by ^{1}H NMR); colorless crystals, mp 398.7–399.7 K (from hexane, heptane or ethyl acetate), lit.: mp 401,[4a] 395–396,[4b] or 398–399[1] K. For the NMR data, see Tables 1 and 3.

Molecular modeling and frequency calculations

Fully-relaxed geometry optimizations of all the molecules were initially carried out by applying the MM+ force field[47] and/or the PM3 method within HyperChem.[48] Further geometry refinement was done at the *ab initio* RHF level with a 6–31G(*d*,*p*) basis set using the Gaussian 98W package[49] (with the six Cartesian components *d* set used for all the heavy atoms). Final DFT level *in vacuo* computations for **1–4** and **7** were performed by the hybrid functional B3LYP method.[50] Moreover, a locally-dense approach[32] was used, by an addition of diffuse orbitals for heteroatoms (Z=O, N), to construct the mixed valence bases marked with 6–31(+)G(*d*,*p*), especially owing to the C=Z bonds and the unshared lone pairs of electrons.[30] Vibrational harmonic wavenumbers were also calculated[31] on these molecular models, to characterize the localized stationary points as true global minima on the correlated surfaces ($N_{imag} = 0$) and to determine the standard Gibbs free-energies ($G^o_{298.15}$, Table S2). Vibrational zero-point energies were scaled with an uniform factor of 0.983[38] to approximately correct for vibrational anharmonicity, basis set truncation and partial neglect of electron correlation. On contrary, an *ab initio* HF approach was used only for the protonated states of **1** (Table S4). All the geometrical calculations and molecular visualizations were carried out with programs PCMODEL,[51] ViewerLite[52] and POVRay.[53] The Intel 3.2 GHz Pentium 4 class PC running under MS Windows® XP Professional SP2 was employed.

NMR spectra prediction

The GIAO[14] DFT-B3LYP/6–311+G(2*d*,*p*) level[54] *in vacuo* calculations of isotropic absolute shieldings (σ_Xs) for oximes **1–4** and **7** were carried out at the equilibrium structures B3LYP/6–31G(*d*,*p*) [and B3LYP/6–31(+)G(*d*,*p*), only for **1**] with the standard routines in Gaussian 98W.[49] The relative chemical shift of a given nucleus X in the molecule is defined as δ_X^{calcd} [ppm] = $\sigma_X^{ref} - \sigma_X^{calcd}$. For the ^{1}H and ^{13}C spectra σ_X^{ref} is always equal to 31.8618 and 182.8589 ppm, respectively, as found analogously on the B3LYP/6–31G(*d*,*p*) model of a dual-reference δ_X standard (TMS of T_d symmetry). Details of *ab initio* calculations for the other species are specified in Table S4. All statistical correlations were performed by linear regression analysis using the MS Excel® 97 spreadsheet.

Supplementary information available

Thermal isomerization of **1** and computational results for **1–9** and DtBK including the GIAO-predicted chemical shifts (Figures S1-S4, Tables S1-S5) (6 pages, PDF). This supplementary material is available free of charge *via* the Internet at http://www.interscience.wiley.com.

REFERENCES

1. Latovskaya SV, Bespalov VYa, Korobitsyna IK. *Zh. Org. Khim.* 1974; **10**: 2336–2342, [oximes of 2,2,4,4-tetramethyl-cyclopentanone (**7**), 2,2-dimethyl-1-oxa-spiro[4.5]decan-3-one (**8**) and 2,2-dimethyl-1-oxa-spiro[4.5]decan-4-one (**9**)].
2. Through this work, the configurational descriptors *E* and *Z* refer to N-OH *syn* and *anti* to the CH_2 group, respectively.
3. Latovskaya SV. The Use of LSRs to Establish the Stereoisomerism of Organic Compounds by ^{1}H NMR Spectroscopy. In *Modern Problems of Organic Chemistry*, vol. 4, Ogloblin KA (ed.). Leningrad University Press: Leningrad, 1975; pp. 141–154, (in Russian).
4. (a) Dupont FG. *Ann. Chim. (Paris) [8]* 1913; **30**: 485–587; (b) Hennion GF, O'Brien JL. *J. Am. Chem. Soc.* 1949; **71**: 2933–2933.
5. Hill RK. *J. Org. Chem.* 1962; **27**: 29–35, and refs therein.

DOI: 10.1002/poc

6. (a) Hill RK, Cullison DA. *J. Am. Chem. Soc.* 1973; **95**: 2923–2927; (b) Grob CA, Ide J. *Helv. Chim. Acta* 1974; **57**: 2562–2571, 2571–2583, and refs therein.
7. (a) Sato T, Inoue T, Yamamoto K. *Bull. Chem. Soc. Jpn.* 1972; **45**: 1176–1179, and refs therein; (b) Yates P, Wong J, McLean S. *Tetrahedron* 1981; **37**: 3357–3363, and refs therein; (c) Bartnik R, Orłowska B. *Polish J. Chem.* 1988; **62**: 151–157, and refs therein; (d) Suginome H, Ohshima K, Ohue Y, Ohki T, Senboku H. *J. Chem. Soc., Perkin Trans. 1* 1994; 3239–3250; (e) (For a review on the photochemical E,Z-isomerization of oximes and related systems see Suginome H. In *CRC Handbook of Organic Photochemistry and Photobiology*, 2nd edn, Horspool W, Lenci F (eds). CRC Press: Boca Raton, FL, 2004; Chapter 94. pp. 94-1–94-55.
8. (a) Stepanenko T, Lapinski L, Sobolewski AL, Nowak MJ, Kierdaszuk B. *J. Phys. Chem. A* 2000; **104**: 9459–9466; (b) Lapinski L, Nowak MJ, Kwiatkowski JS, Leszczynski J. *Photochem. Photobiol.* 2003; **77**: 243–252, and refs therein; (c) Lapinski L, Ramaekers R, Kierdaszuk B, Maes G, Nowak MJ. *J. Photochem. Photobiol. A* 2004; **163**: 489–495.
9. The IR spectroscopic evidence for the direction of these photoisomerizations was provided in Ref. 8b.
10. Ikeda H, Suzue T, Yukawa M, Niiya T, Goto Y. *Chem. Pharm. Bull.* 2002; **50**: 969–971.
11. See *e.g.*, Krstić NM, Bjelaković MS, Dabović MM, Lorenc LB, Pavlović VD, *J. Serb. Chem. Soc.* 2004; **69**: 413–420.
12. (a) Kleinspehn GG, Jung JA, Studniarz SA. *J. Org. Chem.* 1967; **32**: 460–462; (b) Karabatsos GJ, Taller RA. *Tetrahedron* 1968; **24**: 3347–3360; (c) Fox BL, Reboulet JE, Rondeau RE, Rosenberg HM. *J. Org. Chem.* 1970; **35**: 4234–4236; (d) Rondeau RE, Fox BL. U.S. Patent 3,756,779 (1973); (e) Levy GC, Nelson GL. *J. Am. Chem. Soc.* 1972; **94**: 4897–4901; (f) Hawkes GE, Herwig K, Roberts JD. *J. Org. Chem.* 1974; **39**: 1017–1028.
13. (a) Nguyen MT, Raspoet G, Vanquickenborne LG. *J. Am. Chem. Soc.* 1997; **119**: 2552–2562; (b) Nguyen MT, Raspoet G, Vanquickenborne LG. *J. Chem. Soc., Perkin Trans. 2* 1997; 821–825; (c) Mori S, Uchiyama K, Hayashi Y, Narasaka K, Nakamura E. *Chem. Lett.* 1998; **2**: 111–112; (d) Parker WO'N, Jr. *Magn. Reson. Chem.* 1999; **37**: 433–436; (e) Chung Y-M, Rhee H-K. *J. Mol. Cat. A* 2001; **175**: 249–257; (f) Fernández AB, Boronat M, Blasco T, Corma A. *Angew. Chem. Int. Ed.* 2005; **44**: 2370–2373.
14. (a) Wolinski K, Hilton JF, Pulay P. *J. Am. Chem. Soc.* 1990; **112**: 8251–8260, and refs therein; (b) Rauhut G, Puyear S, Wolinski K, Pulay P. *J. Phys. Chem.* 1996; **100**: 6310–6316; (c) Cheeseman JR, Trucks GW, Keith TA, Frisch MJ. *J. Chem. Phys.* 1996; **104**: 5497–5509; (d) Wiberg KB. *J. Comput. Chem.* 1999; **20**: 1299–1303.
15. Further details are given in Supplementary Material section of this paper (Table S5).
16. (a) Smith PAS, Gloyer SE. *J. Org. Chem.* 1975; **40**: 2504–2508; (b) Chęcińska L, Kudzin ZH, Małecka M, Nazarski RB, Okruszek A. *Tetrahedron* 2003; **59**: 7681–7693, and refs therein.
17. Optical transmittance T of Pyrex borosilicate and soda-lime window glass is very similar in this UVA range; $T = 86\%$ at 353 nm and $T = 75\%$ at ~357 nm for the 5- and 6.35-mm polished plates, respectively (*Jobling Laboratory Division Catalogue*, Stone, Staffordshire, 1972. Garden GK. *Characteristics of Window Glass*, CBD-60; Institute for Research in Construction, NRC Canada, December 1964). **Cautionary Note**: Various unexpected photoprocesses are possible to proceed under high-light conditions of sunny days by simple exposure of photolabile systems in Pyrex glassware to laboratory daylight.
18. Hagens G, Wasacz JP, Joullié M, Yates P. *J. Org. Chem.* 1970; **35**: 3682–3685.
19. Bjørgo J, Boyd DR, Watson CG, Jennings WB. *J. Chem. Soc., Perkin Trans. II* 1974; 757–762.
20. Moehrle H, Wehefritz B, Steigel A. *Tetrahedron* 1987; **43**: 2255–2260.
21. Bartnik R, Orłowska B. *Polish J. Chem.* 1988; **62**: 427–431.
22. For checking the ^{1}H NMR data consistency, the spectrum of cyclopentanone oxime was measured giving $\delta_H(OH) = 10.10$ ppm ppm in DMSO-d_6, identical with the reported one.[12a]
23. Bosch A, Brown RK. *Can. J. Chem.* 1968; **46**: 715–728, (compounds **3** and **4**, *i.e.,* 2-methyl- and 2,2-dimethyl-2*H*-acenaphthylen-1-one oximes, respectively).
24. Saitô H, Terasawa I, Ohno M, Nukada K. *J. Am. Chem. Soc.* 1969; **91**: 6696–6703.
25. Obviously, we should keep in mind that **A** was initially in large excess and, additionally, its amount grew gradually owing to the $Z \rightarrow E$ isomerization. As a result, average ^{1}H signals arising from the equilibrium between (*E*)-**1** and (*E*)-$\mathbf{5}^+$ could not vary significantly from those observed for the form (*E*)-**1** alone.
26. Bartnik R, Orłowska B. *Polish J. Chem.* 1988; **62**: 433–443.
27. Heinisch G, Holzer W. *Collect. Czech. Chem. Commun.* 1991; **56**: 2251–2257, and Refs 1–3 therein.
28. (a) See *e.g.*, McInnes AG, Smith DG, Wright JLC, Vining LC, *Can. J. Chem.* 1977; **55**: 4159–4165; (b) Howe RK, Shelton BR. *J. Org. Chem.* 1990; **55**: 4603–4607; (c) Torrini I, Paglialunga Paradisi M, Pagani Zecchini G, Lucente G, Mastropietro G, Spisani S. *J. Peptide Res.* 2000; **55**: 102–109; (d) Holzer W, Hahn K, Brehmer T, Claramunt RM, Pérez-Torralbla M. *Eur. J. Org. Chem.* 2003; 1209–1219; (e) Curtis MP, Bunnelle WH, Pagano TG, Gopalakrishnan M, Faghih R. *Synth. Commun.* 2006; **36**: 321–326.
29. Undoubtedly, the resulting positive NOE effects would be stronger for a properly degassed and sealed sample of oxime **1**. For example, the 4.5% enhancement was found[28c] for the NOH line after saturation of a *syn* α-CH_2 triplet signal of certain pseudopeptide system possessing the *N*-terminal, acyclic oxime fragment (in DMSO-d_6).
30. (a) See *e.g.*, Rauhut G, Pulay P, *J. Phys. Chem.* 1995; **99**: 3093–3100; (b) Alabugin IV. *J. Org. Chem.* 2000; **65**: 3910–3919.
31. Foresman JB, Frisch Æ. *Exploring Chemistry with Electronic Structure Methods*, 2nd edn, Gaussian, Inc.: Pittsburgh, PA 15106, USA, August 1996; Chapter 4, pp. 61–90.
32. The diffuse orbitals augmented locally-dense (mixed) basis set (cf. Chesnut DB, Byrd EFC, *Chem. Phys.* 1996; **213**: 153–158, and refs therein) was used for all heteroatoms to take the relatively diffuse nature of unshared electron lone pairs into account; see (a) Sebag AB, Forsyth DA, Plante MA, *J. Org. Chem.* 2001; **66**: 7967–7973, (N atoms); (b) Migda W, Rys B, *Magn. Reson. Chem.* 2004; **42**: 459–466, (O atoms).
33. Somewhat unexpected and maybe fortuitous, however, is finding that the application of B3LYP/6–31G(*d,p*)-type geometries led to slightly smaller mean deviations of δ_C^{calcd}s *vs* δ_C^{exp}s than those obtained with an extended basis 6–31(+)G(*d,p*); (Table S1). Therefore, in all further calculations only the former double-ζ quality basis set was used.
34. (a) Fabian J, Hartmann H, Noack A. *J. Phys. Org. Chem.* 2003; **16**: 53–62, (S atoms); (b) Adcock W, Peralta JE, Contreras RH. *Magn. Reson. Chem.* 2003; **41**: 503–508, (F atoms).
35. The Pearson coefficient of the correlation, *r*, was used to measure the strength of relationships $\delta_X^{calcd} = f(\delta_X^{exp})$ and a linear regression equation of the type $y_i = ax_i + b + e_i$ (where e_i - error) to mathematically define these relations. For details, see note 16 in Ref. 36.
36. Michalik E, Nazarski RB. *Tetrahedron* 2004; **60**: 9213–9222.
37. Two-nuclear C,H-linear regressions between different δ_Xs for the same molecules were used recently in Ref. 36. For the analysis concerning the δ_Cs only, see Figure S2a.
38. An average ZPE/thermal energy scaling factor of 0.983 was arbitrarily chosen for all the DFT-B3LYP calculations, based mainly on the B3LYP/6-31G(*d*)-derived values: (a) Bauschlicher CW , Jr. *Chem. Phys. Lett.* 1995; **246**: 40–44, (0.980) [or 0.989 for the 6-311+G(3*df*,2*p*) basis]; (b) Wong MW. *Chem. Phys. Lett.* 1996; **256**: 391–399, (0.9804); (c) Scott AP, Radom L. *J. Phys. Chem.* 1996; **100**: 16502–16513, (0.9806).
39. Bordwell FG, Zhang S. *J. Am. Chem. Soc.* 1995; **117**: 4858–4861.
40. The enlargement of this database δ_H^{calcd} *vs* δ_H^{obsd} with the values for (*E*)-**7** found[1] in CCl_4 resulted in small lowering of $r(\delta_H)$ to 0.9985. This effect can by rationalized with the solvent change, as relation of the type $\delta_X^{calcd} = a\delta_X^{obsd} + b$ is strongly solvent dependant.[32b]
41. The HF/6-31G(*d*) distance of 1.553 Å reported in Ref. 13b was fully confirmed in our hand, at this level.
42. Voronov VK, Nesterenko RN, Mikhaleva AI, Kanitskaya LV. *Zh. Strukt. Khim.* 1986; **27**: 163–165; *J. Struct. Chem.* 1986; **27**: 317–319.
43. (a) See *e.g.*, Ribó JM, Serra X, *Org. Magn. Reson.* 1979; **12**: 467–472; (b) Abraham RJ, Chadwick DJ, Griffiths L, Sancassan F. *Tetrahedron Lett.* 1979; 4691–4694; (c) Abraham RJ, Chadwick DJ, Sancassan F. *Tetrahedron* 1982; **38**: 1485–1491; (d) Chiasson

DOI: 10.1002/poc

JB, Jankowski K. In *Lanthanide Shift Reagents in Stereochemical Analysis*, Morrill TC (ed.). VCH Publishers, Inc.: New York, 1986; pp. 19–53.
44. Morrill TC. In *Lanthanide Shift Reagents in Stereochemical Analysis*, Morrill TC (ed.). VCH Publishers, Inc.: New York, 1986; pp. 1–17.
45. Abraham RJ, Mobli M, Ratti J, Sancassan F, Smith TAD. *J. Phys. Org. Chem.* 2006; **19**: 384–392, and refs therein.
46. (a) Newman MS, Reichle WR. *Org. Synth. Coll. Vol.* 1973; **5**: 1024–1025; *Org. Synth.* 1960; **40**: 88–89; (b) The $^{1}H/^{13}C$ NMR spectra of starting ketone 2 were similar to those reported previously (Burke PM, Reynolds WF, Tam JCL, Yates P. *Can. J. Chem.* 1976; **54**: 1449–1453).
47. Hocquet A, Langgård M. *J. Mol. Model.* 1998; **4**: 94–112.
48. *HyperChem® for Windows, Release 4.5*, Hypercube, Inc., Waterloo, Ontario, Canada N2L 3X2, May 1995.
49. Frisch MJ, Trucks GW, Schlegel HB, Scuseria GE, Robb MA, Cheeseman JR, Zakrzewski VG, Montgomery JA ,Jr, Stratmann RE, Burant JC, Dapprich S, Millam JM, Daniels AD, Kudin KN, Strain MC, Farkas O, Tomasi J, Barone V, Cossi M, Cammi R, Mennucci B, Pomelli C, Adamo C, Clifford S, Ochterski J, Petersson GA, Ayala PY, Cui Q, Morokuma K, Malick DK, Rabuck AD, Raghavachari K, Foresman JB, Cioslowski J, Ortiz JV, Baboul AG, Stefanov BB, Liu G, Liashenko A, Piskorz P, Komaromi I, Gomperts R, Martin RL, Fox DJ, Keith T, Al-Laham MA, Peng CY, Nanayakkara A, Challacombe M, Gill PMW, Johnson B, Chen W, Wong MW, Andres JL, Gonzalez C, Head-Gordon M, Replogle ES, Pople JA. *Gaussian 98W, Revision A.9*; Gaussian, Inc.: Carnegie Office Park, Bldg. 6, Pittsburgh, PA 15106, USA, 1998.
50. (a) Lee C, Yang W, Parr RG, *Phys. Rev. B.* 1988; **37**: 785–789; (b) Becke AD. *J. Chem. Phys.* 1993; **98**: 5648–5652; (c) Stephens PJ, Devlin FJ, Chabalowski CF, Frisch MJ. *J. Phys. Chem.* 1994; **98**: 11623–11627.
51. *PCMODEL V. 8.5, Molecular Modeling Software for Windows Operating System, Apple Macintosh OS, Linux and Unix*; Serena Software: Box 3076, Bloomington, IN 47402-3076, USA, August 2003.
52. ViewerLite 5.0, Version Jul 11 2002, Accelrys Inc.; http://www.accelrys.com
53. POV-Ray™ for Windows, Version 3.6.1c by Cason, C.; Persistence of Vision Raytracer Pty. Ltd.: Williamstown, Victoria, Australia, 2004; http://www.povray.org
54. The valence basis set used for this kind of NMR parameter calculations should be of at least triple-zeta quality, as was suggested by Helgaker T, Jaszuński M, Ruud K. *Chem. Rev.* 1999; **99**: 293–352.

DOI: 10.1002/poc